Anaerobic digestion model no. 1-based distributed parameter model of an anerobic reactor : II. Model validation

Tartakovsky, B.; Mu, S. J.; Zeng, Y.; Lou, S. J.; Guiot, S. R.; Wu, P.

Publisher's version / Version de l'éditeur:
https://doi.org/10.1016/j.biortech.2007.07.061
Bioresource Technology, 99, 9, pp. 3676-3684, 2008-06

Available online at www.sciencedirect.com
ScienceDirect
Bioresource Technology 99 (2008) 3676–3684
BIORESOURCE TECHNOLOGY

Anaerobic digestion model No. 1-based distributed parameter model of an anaerobic reactor: II. Model validation

B. Tartakovsky [b], S.J. Mu [a], Y. Zeng [a], S.J. Lou [b], S.R. Guiot [b], P. Wu [a,*]

[a] *Institute of High Performance Computing, 1 Science Park Road, #01-01, The Capricorn, Singapore 117528, Singapore*
[b] *Biotechnology Research Institute, NRC, 6100 Royalmount Avenue, Montréal, Québec, Canada H4P 2R2*

Received 4 May 2006; received in revised form 14 July 2007; accepted 16 July 2007
Available online 21 September 2007

Abstract

In this study, an ADM1-based distributed parameter model was validated using experimental results obtained in a laboratory-scale 10 L UASB reactor. Sensitivity analysis of the model parameters was used to select four parameters for estimation by a numerical procedure while other parameters were accepted from ADM1 benchmark simulations. The parameter estimation procedure used measurements of liquid phase components obtained at different sampling points in the reactor and under different operating conditions. Model verification used real time fluorescence-based measurements of chemical oxygen demand and volatile fatty acids at four sampling locations in the reactor. Overall, the distributed parameter model was able to describe the distribution of liquid phase components in the reactor and adequately simulated the effect of external recirculation on degradation efficiency. The model can be used in the design, analysis and optimization of UASB reactors.

Keywords: Distributed parameter model; ADM1; UASB reactor; Anaerobic digestion; Multiwavelength fluorometry

1. Introduction

An ADM1-based distributed parameter model (ADM1d) was proposed by Mu et al. (submitted for publication) to simulate anaerobic reactors with significant axial gradients, such as in upflow anaerobic sludge bed (UASB) reactors. ADM1d was compared with ADM1, which uses the assumption of ideal mixing. This comparison was based on benchmark simulations proposed by Rosen and Jeppsson (2002). Overall, the comparison showed that in addition to such factors as organic load and hydraulic retention time, the degradation efficiency of UASB reactors depends on upflow velocity and this factor should be considered in reactor modeling. Significant axial gradients of liquid phase components were predicted to exist in a wide range of operating conditions. The capacity of the distributed parameter model to take into account these factors makes ADM1d a useful tool in UASB reactor design and optimization.

In this study, the distributed parameter model was validated using experimental results obtained in a laboratory-scale UASB reactor. The hydraulic characterization of this reactor showed that the dispersion coefficient was position-dependent (Zeng et al., 2005). Consequently, the dependence of the dispersion coefficient on reactor position was added to the ADM1d equations. A parameter estimation procedure was then carried out using measurements of liquid phase components at different reactor locations and off-gas measurements.

Furthermore, the predictive capacity of ADM1d was validated by comparing model outputs with real time measurements of chemical oxygen demand (COD) and volatile fatty acids (VFAs) obtained using the technique of multiwavelength fluorometry (Morel et al., 2004). Notably, a combination of real time measurements of COD and VFA concentrations at different sampling locations in the

* Corresponding author.
E-mail address: wuping@ihpc.a-star.edu.sg (P. Wu).

0960-8524/$ - see front matter © 2007 Elsevier Ltd. All rights reserved.
doi:10.1016/j.biortech.2007.07.061

Nomenclature

a, b, D_0 parameters of axial dispersion model Eq. (2)
D_x biomass axial dispersion coefficient, $m^2\ h^{-1}$
C^{cal}, C^{exp} normalized calculated and measured concentrations, respectively
$k_{m,ac}$, $k_{m,pr}$, $k_{m,c4}$ maximum specific uptake rates of acetate, propionate, and butyrate, respectively, kg COD m^{-3}
$k_{m,aa}$, $k_{m,fa}$, $k_{m,su}$ maximum specific uptake rates of amino acids, long chain fatty acids, and sucrose, respectively, kg COD m^{-3}
k_{La} mass transfer coefficient, d^{-1}
$K_{S,ac}$, $K_{S,pr}$, $K_{S,c4}$ half saturation constants of acetate, propionate, and butyrate, respectively, d^{-1}
N_{samp} number of samples
T dimensionless sensitivity value
x_{max}, x_{min}, β parameters for calculating biomass distribution
p kinetic parameter
u upflow velocity, m h^{-1}
w weight constant
η dimensionless normalized axial position

reactor with a process model yields a powerful tool, which can be used in advanced process control and optimization.

2. Methods

2.1. Experimental setup

Experiments were carried out in a 10.4 L Plexiglas reactor with an internal diameter of 14.3 cm (Fig. 1). The reactor was equipped with a water jacket for temperature control, a pH control system, and an external recirculation loop. The flow rate of biogas being generated was measured by an electronic bubble counter. The methane and carbon dioxide content of the biogas were measured online using a gas analyzer (Ultramat 22P, Siemens, Germany) interfaced with a computer. The reactor pH was measured using a pH-meter (model 5997, Cole-Parmer, Vernon Hills, IL, USA) and maintained at pH 7 by computer-controlled addition of 0.5 N NaOH.

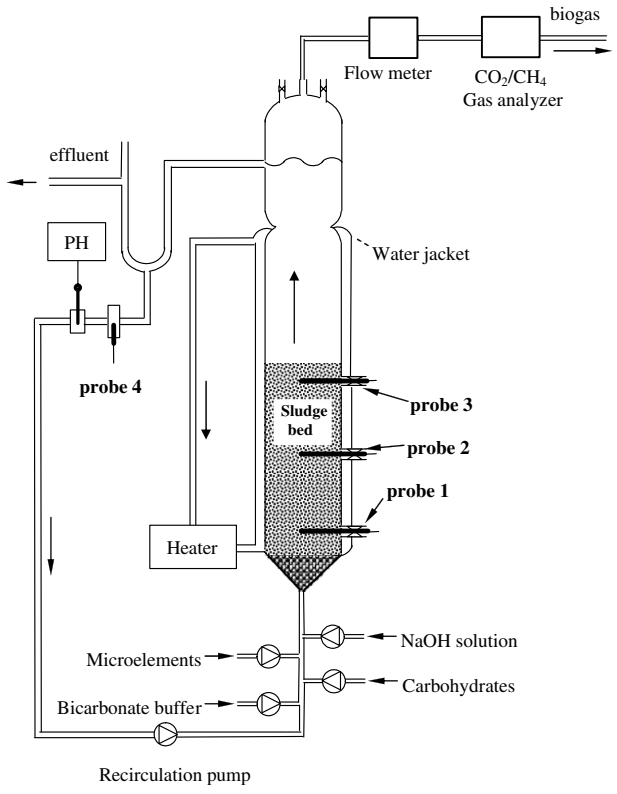

Fig. 1. A schematic diagram of the experimental setup. Sampling devices used for fluorescence measurements at different reactor heights are shown as probes 1–4.

The reactor was inoculated with granular anaerobic sludge (A. Lassonde Inc., Rougemont, Quebec, Canada). The average volatile suspended solids (VSS) content of the inoculum sludge was 50 kg m^{-3}. The temperature was maintained at 30 °C throughout the experiment. The influent stream contained bicarbonate buffer (0.68 kg m^{-3} of $NaHCO_3$ and 0.87 kg m^{-3} of $KHCO_3$), microelements and synthetic wastewater. A stock solution of synthetic wastewater contained (in kg m^{-3}): sucrose 99; butyric acid 48; yeast extract 60; ethanol (95%) 35; KH_2PO_4 3; K_2HPO_4 3.5; NH_4HCO_3 34. The stock solution was diluted according to the desired organic load to obtain the target wastewater strength. The microelements solution contained (in g m^{-3}): $AlK(SO_4)\cdot 12H_2O$ 0.1, H_3BO_3 0.17, $Ca(NO_3)_2\cdot 4H_2O$ 88.3, $Co(NO_3)_2\cdot 6H_2O$ 1.2, $Cu(SO_4)$ 0.05, $Fe(SO_4)\cdot 7H_2O$ 9.0, $MgSO_4$ 32.6, $Mn(SO_4)\cdot H_2O$ 2.5, $Na_2(MoO_4)\cdot 2H_2O$ 0.38, $NiSO_4\cdot 6H_2O$ 0.12, Na_2SeO_4 0.21, $ZnSO_4\cdot 7H_2O$ 0.58.

A hydraulic retention time of 10 h was maintained throughout the experiment by adjusting the feeding rate of bicarbonate buffer. The organic load and the recirculation rate were changed each seven days, as described in Table 1. Four different combinations of organic load and upflow velocity were used. The concentrations of COD,

Table 1
Experimental conditions

Experiment conditions	Phase #1	Phase #2	Phase #3	Phase #4
Duration (day)	(1–7)	(8–14)	(15–22)	(22–25)
Recirculation/influent ratio	1	12	4	4
Upflow velocity (m h^{-1})	0.15	0.83	0.32	0.32
OLR (kg COD m_R^{-1} m^{-3} d^{-1})	6	6	6	10

Reactor was operated at a temperature of 35 °C and an influent flow rate of 0.576 $m^3\ d^{-1}$.

VFAs, and VSS were measured periodically at the four reactor levels shown in Fig. 1. On-line measurements of soluble COD and total VFA were carried out at the same reactor positions.

2.2. On-line fluorescence measurements

Fluorescence measurements were carried out using a multi-wavelength fluorometric system consisting of a light source connected to an R400-7 fiber optic reflection probe, and coupled to a USB2000 CCD array fiber optic spectrometer (Ocean Optics Inc., Dunedin, FL, USA). The spectrometer had a spectral range of 250–800 nm and a resolution of 0.9 nm. A UV LED light source (LS-450 with a 380 nm UV LED) was used for on-line substrate measurements (Ocean Optics Inc., Dunedin, FL, USA). A PC equipped with a Celeron 2.6 GHz processor was used for light source control and spectra acquisition. Fluorescence spectra were acquired in a range of 400–800 nm at 10 min intervals with background acquisition prior to each fluorescence measurement followed by background subtraction from each acquired fluorescence spectrum. A spectrometer integration time of 2000 ms and an average of 10 spectra were used for data acquisition.

To follow substrate distribution in the reactor, fluorescence sampling devices were installed at four locations within the reactor (Fig. 1). Each sampling device consisted of a perforated plastic rod, which extended into the reactor center, a 12 rpm peristaltic pump (Cole-Parmer, Chicago, IL, USA) and a liquid return line (Fig. 1, enlargement). The liquid recirculation rate of the sampling pumps was 15 mL min^{-1}. Sampling devices were equipped with fiber optic probes for fluorescence measurements and sampling ports for off-line measurements. The fiber optic probes were inserted perpendicular to the flow. The three sampling devices were installed at heights of 2.5, 13.0, and 34.5 cm from the base of the reactor, and corresponded to the bottom, middle and top of the anaerobic sludge bed, respectively. The effluent substrate concentrations were measured with a fiber-optic reflection probe installed in the external recirculation line of the reactor and corresponded to a distance of 65 cm from the reactor base (Fig. 1, probe #4).

COD and VFA concentrations were calculated by partial least squares (PLS) regression models calibrated using off-line analytical measurements. Fluorescence signals are proportional to the amount of fluorophores in the liquid, such as proteins and amino acids. This implies that the COD and VFA concentrations were measured by correlating these parameters with the concentrations of the fluorophores. A detailed description of the calibration procedure can be found elsewhere (Morel et al., 2004). Details on rhodamine (conservative tracer) measurements are given in Zeng et al. (2005).

2.3. Analytical measurements

Liquid samples were collected and centrifuged for 10 min at 10,000 rpm to remove solids. The supernatant was then analyzed for COD and VFA content. Biomass samples were collected at the end of each experimental phase and the concentration of VSS was determined. Concentrations of VSS and COD were determined according to standard methods (APHA et al., 1995). The amounts of VFAs were measured using a gas chromatograph (Sigma 2000, Perkin–Elmer, Norwalk, USA) equipped with a 91 cm × 4 mm i.d. glass column packed with 60/80 Carbopack C/0.3% Carbopack 20 NH_3PO_4 (Supelco Canada Ltd., Oakville, ON). The column temperature was maintained at 120 °C, while the injector and detector temperature was 200 °C. The carrier gas was nitrogen.

For both COD and VFA measurements, the coefficient of variation attributed to the analytical procedures did not exceed 5%. However, errors associated with sampling procedures led to an overall variation coefficient of up to 15%, in particular for low levels of COD and VFAs. Owing to the heterogeneity of sludge samples, VSS estimations had a variation coefficient of up to 20%.

3. Results and discussion

3.1. Sensitivity analysis

The distributed parameter model described in the first part of this two-part paper used the same kinetic parameters as ADM1 (Batstone et al., 2000a,b, 2002). However, reactor configuration and operating conditions used in this study were different from those of the ADM1 benchmark simulations (Rosen and Jeppsson, 2002) thus re-estimation of the model parameters was required.

Owing to a large number of ADM1d parameters, estimation of all the parameters would require a significantly broader pool of experimental results to avoid ill-conditioning of the parameter estimation (minimization) problem (Kesavan and Law, 2005). The problem of ill-conditioning was avoided by restricting the number of identifiable parameters. Although all parameters affected model outputs, the significance differed from one to another. The stoichiometric parameters of the model are independent of reactor configuration and should respect biotransformation mechanisms. Also, the synthetic wastewater used in the experiment did not contain solid materials, had a low nitrogen content, and the reactor was equipped with a pH control system. Consequently, the stoichiometric, disintegration, and hydrolysis constants as well as model parameters describing the inhibition effect of inorganic nitrogen and the pH effect were not re-estimated. Overall, parameters considered for re-estimation were the half saturation constants ($K_{s,i}$) and maximum specific uptake rates ($k_{m,i}$) of soluble substrates contributing to total soluble COD (sucrose, amino acids, long chain fatty acids, butyrate, propionate, and acetate). In addition, the gas transfer coefficient, which is dependent on reactor configuration, was considered for re-estimation. The 18 model parameters given in Table 2 were considered for parameter estimation, but this number had to be further reduced.

Table 2
Model parameters used for sensitivity analysis and results of parameter estimation

Parameter	Benchmark values	Initial guess	ADM1d values	Units
$k_{m,aa}$	50	–	–	d^{-1}
$K_{S,aa}$	0.3	–	–	kg COD m^{-3}
$k_{m,fa}$	6	–	–	d^{-1}
$K_{S,fa}$	0.4	–	–	kg COD m^{-3}
$k_{m,c4}$	20	6	2.3[a]	d^{-1}
$K_{S,c4}$	0.2	–	–	kg COD m^{-3}
$k_{m,pr}$	13	5	2.4[a]	d^{-1}
$K_{S,pr}$	0.1	–	–	kg COD m^{-3}
$k_{m,su}$	30	–	–	d^{-1}
$K_{S,su}$	0.5	–	–	kg COD m^{-3}
$k_{m,ac}$	8	5	1.0[a]	d^{-1}
$K_{S,ac}$	0.15	–	–	kg COD m^{-3}
k_{La}	200	–	120[a]	d^{-1}
$K_{S,IN}$	0.0001	–	–	M
$K_{I,nh3}$	0.0018	–	–	M
$K_{I,h2,fa}$	5e−6	–	–	kg COD m^{-3}
$K_{I,h2,c4}$	1e−5	–	–	kg COD m^{-3}
$K_{I,h2,pro}$	3.5e−6	–	–	kg COD m^{-3}
D_x	–	–	0.0024[b]	$m^2\ d^{-1}$
x_{max}	–	–	100[b]	kg COD m^{-3}
x_{min}	–	–	0[b]	kg COD m^{-3}
β	–	–	5[b]	–
D_0 (Eq. (2))	–	–	24[c]	$m^2\ d^{-1}$
a (Eq. (2))	–	–	1.11[c]	–
b (Eq. (2))	–	–	0.009[c]	–

Other ADM1d parameters are given in Mu et al. (submitted for publication). Hydraulic parameters were estimated by Zeng et al. (2005).
[a] Estimated in this study.
[b] Assumed.
[c] Zeng et al. (2005).

Sensitivity analysis has been widely applied to reduce model complexity, determine the significance of model parameters and identify dominant parameters (Makinia and Wells, 2000; Bernard et al., 2001; Degenring et al., 2004). In this study, the local relative sensitivity analysis method (Dochain and Vanrolleghem, 2001) was employed to calculate sensitivity functions. The sensitivities were quantified in terms of the variation of measurable process variables under the perturbation of model parameters in their neighbourhood domain.

The numerical calculation of sensitivity functions used the finite difference approximation (Dochain and Vanrolleghem, 2001). The value of the perturbation factor δ was chosen such that the differences between the resulting sensitivity values of different parameters can be detected

$$T_{ij} = \frac{\partial c_i/c_i}{\partial p_j/p_j} \approx \frac{(c_i(t,p_j+\delta p_j)-c_i(t,p_j))/c_i(t,p_j)}{\delta p_j/p_j} \quad (1)$$

where T_{ij} is the dimensionless sensitivity value of the ith measurement with respect to the jth model parameter; c_i ($i=1,\ldots,6$) denotes the ith process variable (effluent concentrations of soluble COD, acetate, propionate, butyrate, biogas flow rate, and methane percentage, respectively); p_j is the jth model parameter, $j=1,\ldots,18$.

For the local relative sensitivity analysis, a reference value is required as a starting point for evaluating the perturbation factor. Simulations using ADM1 benchmark values showed greater than 50% discrepancies between the experimental results and the model predictions. Thus, the values of some model parameters were manually changed to obtain a better fit. These values are listed in Table 2. The perturbation factor δ was set to 1% for all the calculations and the local sensitivity values were evaluated. The resulting local sensitivity values of the four process variables (soluble COD, acetate, propionate, and methane percentage) to the 18 model parameters shown in Fig. 2.

Sensitivity functions were similar for soluble COD, acetate, propionate (Fig. 2a–c), and butyrate (results not shown). Maximum specific uptake rates and half saturation constants of acetate ($k_{m,ac}$, $K_{S,ac}$), propionate ($k_{m,pr}$, $K_{S,pr}$), and butyrate/valerate ($k_{m,c4}$, $K_{S,c4}$) had the largest impact in comparison to such parameters as the maximum specific uptake rates of amino acids ($k_{m,aa}$), long chain fatty acids ($k_{m,fa}$) and sucrose ($k_{m,su}$). The sensitivity to half saturation constants was similar to that for respective maximum specific uptake rates. The mass transfer coefficient (k_{La}) had a larger impact than the other parameters (Fig. 2d) and was also selected for re-estimation. Similar sensitivity functions were obtained for biogas flow rate (results not shown).

As discussed above, accurate estimations of half saturation constants would require a much larger set of experimental results including kinetic tests at substrate concentrations comparable with the values of half saturation constants. Meanwhile, in the reactor experiment the substrate concentrations were above those corresponding to the half saturation constants. Consequently, half saturation constants were kept unchanged from their benchmark values. In summary, $k_{m,ac}$, $k_{m,pr}$, $k_{m,c4}$, and k_{La} were selected for re-identification, while all other parameters were accepted from ADM1 benchmark simulations.

3.2. Position-dependent dispersion coefficient

A tracer test technique has been used to estimate hydraulic parameters of the experimental setup. In our previous work, the concentrations of a fluorescent tracer rhodamine were measured on-line at four locations in the reactor (Zeng et al., 2005). The measurements were carried out with different combinations of organic loads and external recirculation rates and then used in estimating parameters of the transport model. Data analysis showed that the dispersion coefficient was position-dependent within the sludge bed and it was constant in the liquid above the sludge bed. The outputs of the transport model had low sensitivity to variations of the dispersion coefficient in the liquid zone and to the bypass rate in the sludge bed zone. Moreover, the bypass coefficient was estimated to be close to zero. The following equation was used for calculating the dispersion coefficient (D):

$$D = D_0 \times u^a \times b^\eta \quad (2)$$

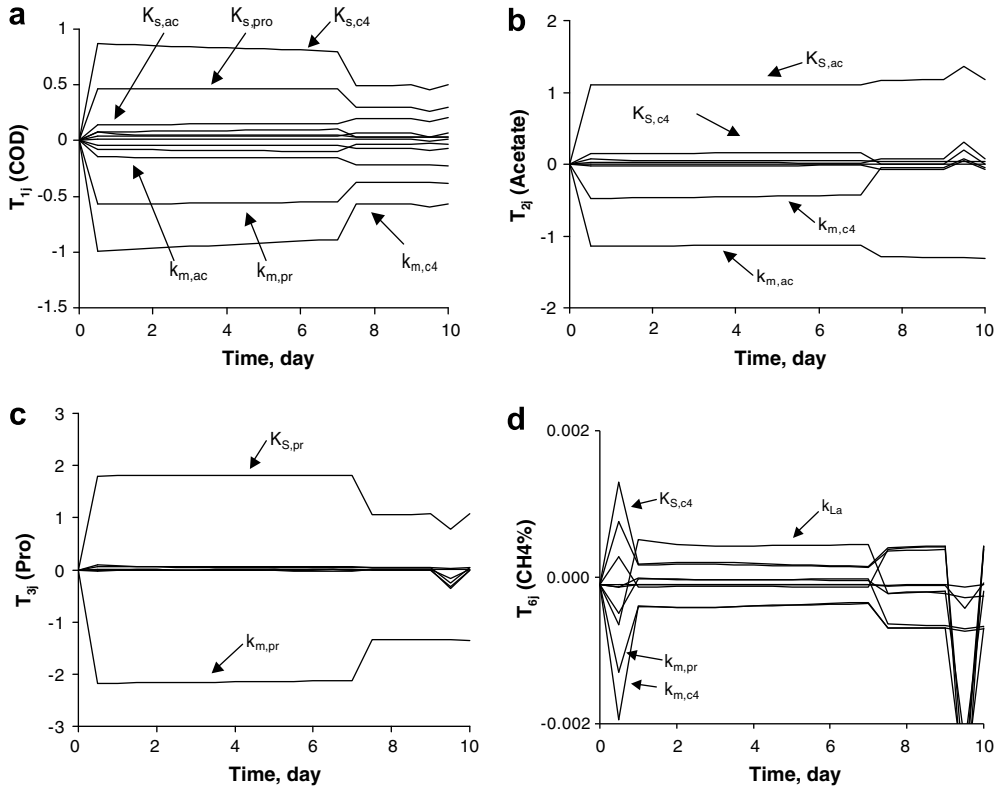

Fig. 2. Sensitivity analysis of model parameters on soluble COD (a), acetate (b), propionate (c), and methane percentage (d).

where, D_0, a and b are parameters with estimated values of 24 $m^2\,d^{-1}$, 1.11 and 0.009, respectively (Table 2); u is the upflow velocity, $m\,h^{-1}$; η is the dimensionless normalized axial position. Thus, the dispersion coefficient in the sludge bed zone decreased going from the bottom to the top of the sludge bed. This change was nearly linear and was dependent on the liquid upflow velocity. It was hypothesized that dense packing of biomass granules at the bottom of the sludge bed resulted in a higher apparent linear upflow velocity and, consequently, in spatial variation of the dispersion coefficient. Although Eq. (2) was initially developed for the sludge zone of the two-compartment model, the estimation of the dispersion coefficient in the liquid zone showed that it was equal to the value at the top of the sludge bed zone (Zeng et al., 2005). Consequently, Eq. (2) was added to ADM1d and used for calculations of D at all reactor locations.

3.3. Parameter estimation

ADM1d parameters selected by the sensitivity analysis were estimated by minimizing the difference between the measurements and model outputs. Measurable process variables included soluble COD, butyrate, propionate, and acetate concentrations. These variables were measured at four sampling ports located along the reactor height. Also, biogas flow rate and methane concentration in the biogas were measured. The following objective function (F_{obj}) was used for parameter estimation:

$$F_{obj} = \sum_{i=1}^{6} w_i \left(\sum_{j=1}^{4} \sum_{k=1}^{N_{samp}} \left(\left(C_{i,j,k}^{cal} - C_{i,j,k}^{exp} \right) / C_{i,j,k}^{exp} \right)^2 \right) \quad (3)$$

where, $C_{i,j,k}^{cal}$ and $C_{i,j,k}^{exp}$ are the normalized calculated and the measured values of the ith process variable at the jth sampling port along the reactor height and at the kth sampling time during the experiment; N_{samp} is the number of samples, $N_{samp} = 38$; w_i is the weight constant of the ith process variable.

The Simplex minimization algorithm (Nelder and Mead, 1965) was used to solve the minimization problem in Eq. (3). The values of 100 and 0 kg COD m^{-3} were assigned to x_{max} and x_{min} variables in the biomass distribution model, respectively, and all weight constants in Eq. (3) were set to 1. With these values the sludge distribution was similar to that observed in the experiment. The model was solved by a finite difference method with 20 internal points. Because the pH of the reactor was maintained at 7 by the pH controller, the model equations were simplified by setting pH to a constant value, i.e. the ion balance equations were excluded. The values of model parameters obtained after 300 iterations of the minimization algorithm are listed in Table 2.

A comparison of the resulting parameter values with those of ADM1 (Table 2) showed that the estimated maximal transformation rates $k_{m,ac}$, $k_{m,pr}$, and $k_{m,c4}$ were smaller than their respective ADM1 values. The estimated k_{La} was also smaller than the ADM1 value. The differences in kinetic constants can be attributed to differences in

sludge composition, in particular to a different ratio of inert organic materials to microorganisms.

Fig. 3 showed measured and calculated values of the process variables. Four distinct parts corresponding to 4 experimental phases can be observed. Overall, model outputs followed the experimental results with reasonable accuracy. A comparison of measured and predicted COD concentrations at the bottom, middle, and top of the sludge bed, and in the effluent showed qualitatively similar trends, although VFA concentrations at the bottom of the sludge bed were significantly underestimated throughout phase #1 (Fig. 3). This error in estimating COD and VFA concentrations can be attributed to a combination of two factors. Large standard deviations were obtained when estimating dispersion coefficient parameters in Eq. (2) at low upflow velocities (Zeng et al., 2005). This error in D estimation might influence the accuracy of model predictions at low values of u. Furthermore, almost constant and close to neutral pH values were predicted along the height of the reactor by acid–base equilibria equations of ADM1. Consequently, free-acid inhibition at the reactor base was insignificant leading to an overestimation of VFA transformation rates.

It should be noted that the measurements exhibited high variability, in particular throughout phase #1. Examination of liquid phase components (COD and acetate in Fig. 3) showed that when the recirculation to influent ratio increased from 1 (phase #1) to 12 (phase #2), the differences between concentrations at the sludge bed bottom and in the effluent decreased. When the recirculation to influent ratio was decreased from 12 (phase #2) to 4 (phase #3), these differences were again observable but less pronounced than in phase #1. Finally, an increase of OLR from 6 to 10 kg COD m_R^{-3} d^{-1} in phase #4 caused an increase of COD and VFA concentrations at all sampling points.

A comparison of measured and calculated biogas flow rates and methane concentration (Fig. 3) also showed reasonable agreement. Biogas flow rate slightly increased with an increase in the recirculation rate (phase #1 to phase #2), and decreased when the recirculation rate was decreased (phase #2 to phase #3). As expected, an increase in the OLR (phase #3 to phase #4) caused a significant increase in biogas production. Finally, both increased recirculation ratio and increased OLR resulted in a decrease in methane percentage.

A more detailed look at the axial distribution of substrates and microorganisms in the reactor predicted by the model showed that experimentally observed distribution of soluble COD and total VFAs along the reactor height were followed (Fig. 4). The results in Fig. 4 corresponded to the end of each experimental phase described in Table 1. The gradients of COD and VFAs were the largest in phase #1, which was carried out at the lowest recirculation rate. These gradients were adequately described by the model with determination coefficients (R^2) of 0.97 and 0.92 for COD and total VFAs, respectively. The concentration gradients became less pronounced with an

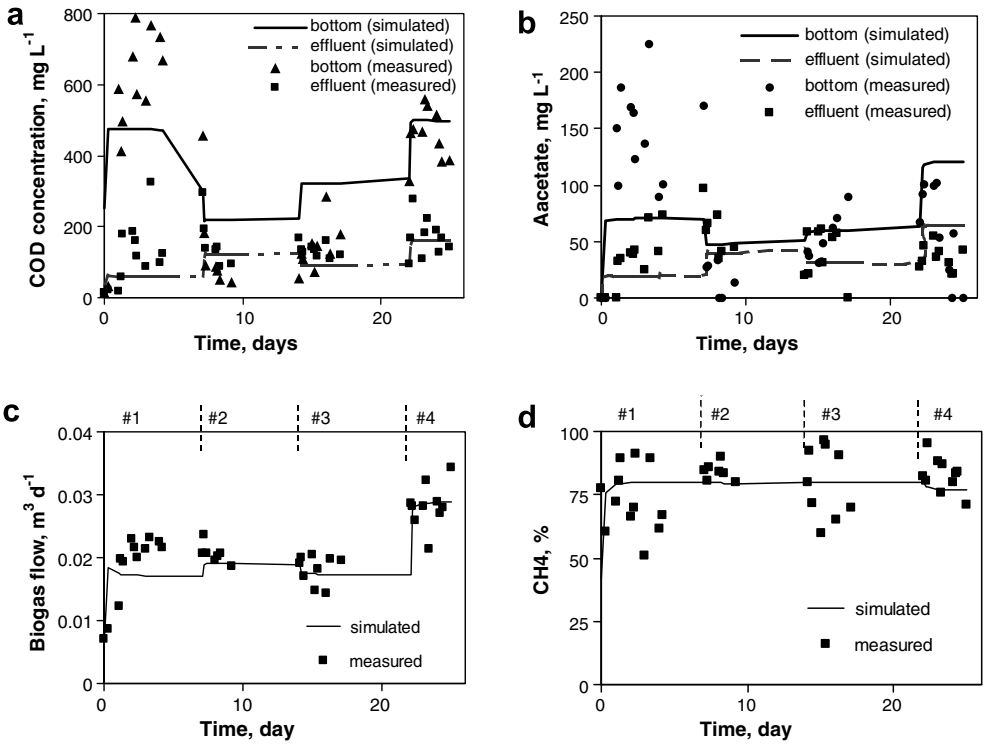

Fig. 3. Comparison of measured and predicted concentrations of soluble COD (a), acetate (b), biogas flow rate (c) and methane percentage (d) values. Concentrations were measured at 2.53, 12.65, 33.53 and 63.27 cm from the bottom of the reactor. Only the results obtained at 2.53 and 63.27 cm are shown. Four experimental phases are indicated by dashed vertical lines.

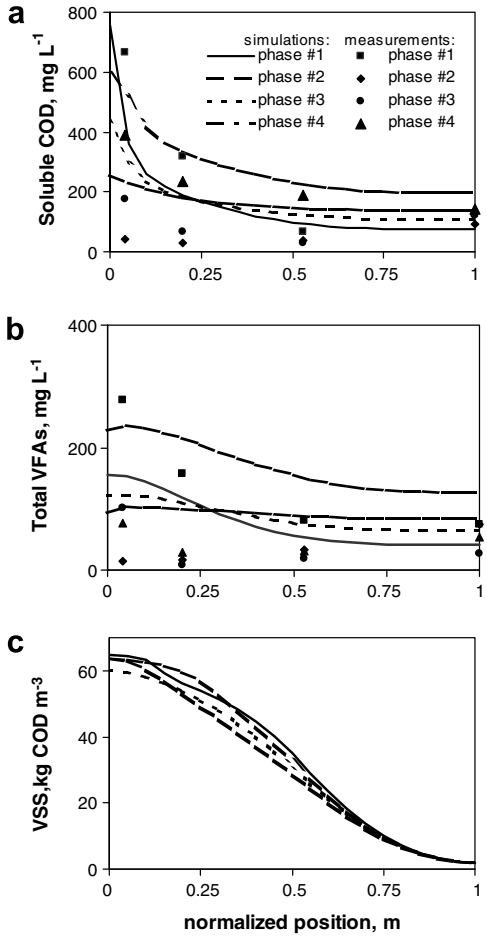

Fig. 4. A comparison of computed (lines) and measured (symbols) spatial distribution of soluble COD (a) and total VFAs (b) at the end of each experimental phase. Computed distribution of VSS is shown in panel (c). Notations are as in panel (a).

increased recirculation rate (phase #2) and the measurements became more scattered resulting in R^2 values below 0.5. In phase #3 the gradients increased again because of increasing OLR and a better agreement between the measurements and the model outputs was obtained (R^2 above 0.6). Obvious discrepancies of the simulated and experimental profiles of CODs and VFAs at the lowest recirculation rate can be attributed to high variations of the measurements and to the fact that only four model parameters were estimated, while all other parameters, including the half saturation constants, were taken from the benchmark study. Meanwhile, sensitivity analysis showed the model outputs were sensitive to both variations of maximum uptake rates and half saturation constants (Fig. 2a–c).

While a detailed analysis of the composition of the anaerobic sludge was not done, a total amount of microorganisms can be calculated using a conversion factor of 1.4 kg COD per kg VSS. The calculated profiles of biomass in the reactor are shown in Fig. 5. These values agreed with the measurements carried out at the end of phase #1, which gave a VSS of 47–52 g COD m^{-3} at the reactor bottom and 13 g COD m^{-3} at the top of the sludge bed. Throughout the experiment VSS concentration at the bottom of the sludge bed increased and reached 80–90 g COD m^{-3} by the end of phase #4. Also, phase #1 corresponded to the lowest predicted effluent biomass concentration of 1.96 kg COD m^{-3} because of better settling. The effluent biomass concentration was predicted to increase with increasing recirculation rate because of higher washout.

3.4. Model verification and analysis of model predictions

Model verification was carried out by comparing model outputs with the values of soluble COD and total VFAs measured on-line by the multi-wavelength fluorometric system (Lou et al., 2006). The on-line measurements used for the comparison were obtained between days 4 and 9 and included a transition between phases #1 and #2 due to the change in upflow velocity.

The comparison of model predictions and on-line measurements of soluble COD and total VFA concentrations at three reactor positions are shown in Fig. 5a and b, respectively. It can be seen that ADM1d was capable of predicting process dynamics and that the accuracy of COD predictions was better than that of VFAs. As discussed above, the model underestimated free-acid inhibition of VFA transformation, thus resulting in lower than measured concentrations of VFAs at the base of the reactor.

Notably, proteins exhibit strong fluorescence, while VFAs are weak fluorophores. Consequently, the VFA measurements were based on the correlations with the fluorescent components of the liquid. The model predicted a fast decrease in COD concentration at the reactor base upon increasing the recirculation rate. This transition was also observed experimentally (day 7 in Fig. 5), however the measurements showed that the decrease in the COD concentration was followed by a temporary COD increase between days 7 and 8. Apparently, this was caused by fluctuations in the pH because of the proportional algorithm for pH control. Importantly, the fluctuations in the pH caused no observable changes in the effluent concentrations of COD and VFA, while the VFA peak at the bottom of the sludge bed was significant (Fig. 5b, day 7.5). Since ADM1d assumed a constant reactor pH, these variations in COD and VFA concentrations were not followed by the model. Nevertheless, the measurements signified the importance of real time measurements at several reactor locations. The existence of a low pH and high VFA zone at the bottom of the sludge bed can lead to propagation of the acidogenic zone and eventually to failure of the reactor. On-line measurements would allow for early diagnosis of the overload events, while the model can be used to estimate the significance of the overload.

Evidently, the recirculation flow rate had a significant effect on the axial distribution of liquid phase components and hence on effluent concentrations. At recirculation-to-influent ratios above 4, mixing was significantly improved

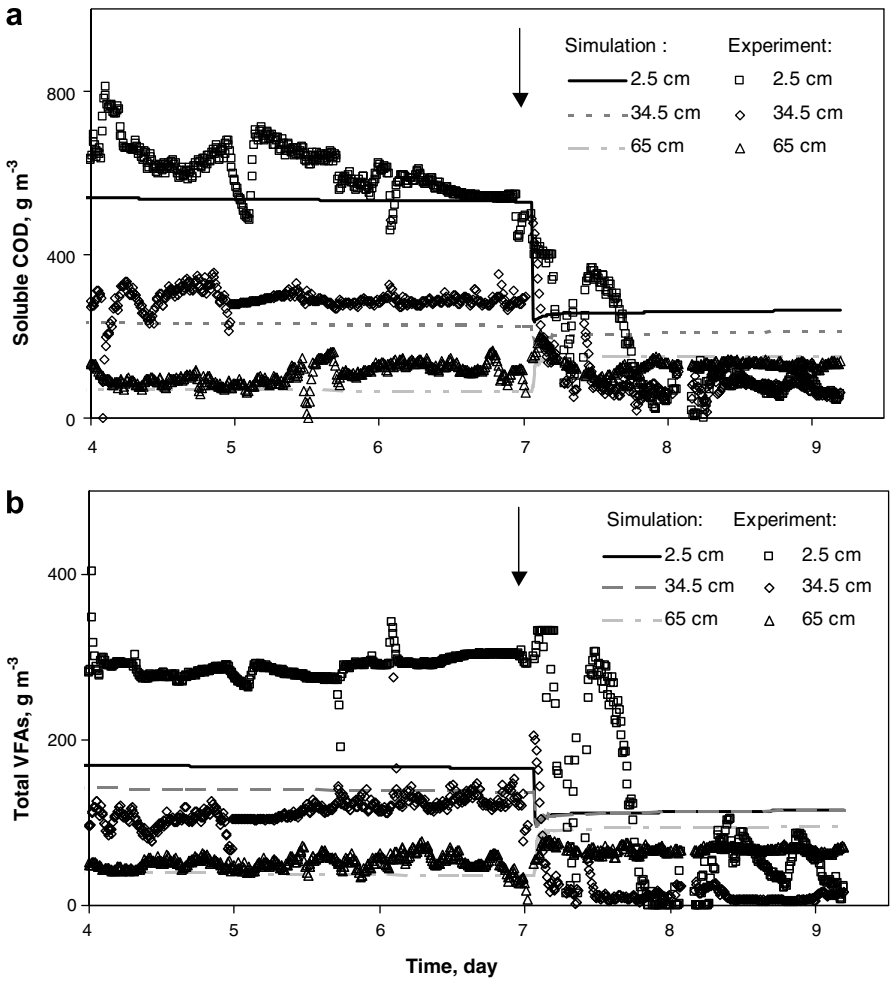

Fig. 5. ADM1d predictions and on-line measurements of soluble COD and total VFA concentrations between days 4 and 9 of the experiment. Arrows indicate an increase of u from 0.15 to 0.83 m h^{-1}. Legend shows distances from the base of the reactor.

and led to less pronounced axial gradients. Better mixing, however, resulted in somewhat higher effluent COD concentrations and increased biomass washout. While better mixing might improve the overall efficiency of the reactor in cases of substrate or pH-related toxicity, under normal operating conditions a lower recirculation rate can be advantageous. The computed relationships between the recirculation rate, maximal attainable organic load, and COD removal efficiency are plotted in Fig. 6. These curves were calculated by setting a constant recirculation to influent ratio and increasing OLR until reactor failure was observed. At each combination of recirculation and OLR values the model was integrated for a period of 10 days. Thus, the OLR and removal efficiency values shown in Fig. 6 correspond to maximal attainable operating conditions at a given recirculation rate.

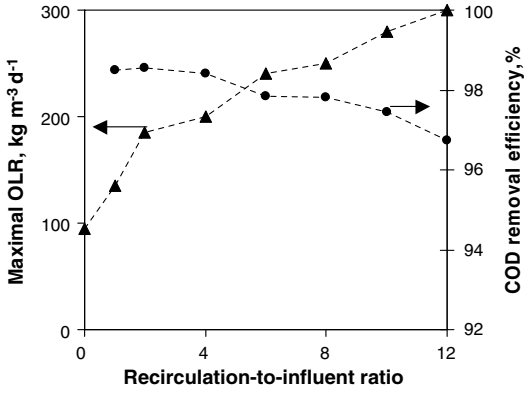

Fig. 6. Computed COD removal efficiency and maximal attainable organic loading rate at different recirculation-to-influent ratios.

It can be seen that low recirculation rates were predicted to result in a higher COD removal efficiency. At the same time, the failure of an overloaded reactor was postponed if higher recirculation rates were used. In summary, high recirculation rates led to improved reactor stability while the removal efficiency declined and biomass washout increased. It would be beneficial to adopt an appropriate recirculation-to-influent ratio in order to dilute the influent wastewater. This helps to avoid the accumulation of toxic substrates and VFAs at the bottom of the reactor (Sam-Soon et al., 1991; Torkian et al., 2003; Mshandete et al., 2004). It should be noted that the simulation results in

Fig. 6 did not take into account possible effects of liquid bypass in the sludge bed.

4. Conclusions

In this work, a distributed parameter model was validated using experiments in a laboratory UASB reactor with an external recirculation loop. Sensitivity analysis showed that maximum specific uptake rates, half saturation constants, and the gas–liquid transfer constant were the most sensitive parameters. The four parameters chosen for estimation were the maximum specific uptake rates of acetate, propionate and butyrate ($k_{m,ac}$, $k_{m,pr}$, $k_{m,c4}$) and the gas–liquid transfer constant (k_{La}). These parameters were estimated by minimizing the difference between ADM1d outputs and the experimental measurements. Overall, ADM1d satisfactorily described effluent concentrations of COD and VFAs under different organic loads and recirculation rates, and was able to simulate COD and VFA gradients in the reactor. Unlike ADM1, which assumes ideal mixing in the reactor and hence homogeneous distribution of components in the reactor, ADM1d is capable of predicting the existence of COD and VFA gradients along the reactor height. Furthermore, the simulated dynamic response to changing operating conditions agreed with real time fluorescence-based measurements of COD and VFA concentrations. Both the simulations and measurements underlined the importance of a comprehensive monitoring of UASB reactors, especially at different locations in the reactor. Fluorescence-based measurements used in this work for model validation can be seen as a proof that real time COD and VFA measurements can be successfully accomplished.

The distributed parameter model developed in this study can be used in the design, analysis and optimization of UASB reactors. Owing to its ability to model spatial distribution of liquid phase components, ADM1d has the potential to be integrated into a process control system. The interesting topics for future studies are the influence of recirculation rate on the substrate and pH distribution in the reactor and process optimization by adjusting the recirculation rate.

Acknowledgements

This work is funded by the NRC-A*STAR Collaborative Research Program for BRI-NRC, Canada and the Singapore-NRC Joint Research Programme (A*STAR Grant) for IHPC, Singapore. The authors appreciate the suggestions of Dr. Darwin Lyew on improving the readability of this manuscript. This is NRC paper #49083.

References

APHA, AWWA, WEF, 1995. Standard Methods for the Examination of Water and Wastewater. American Public Health Association, Washington, DC.

Batstone, D.J., Keller, J., Angelidaki, I., Kalyuzhnyi, S.V., Pavlostathis, S.G., Rozzi, A., Sanders, W.T.M., Siegrist, H., Vavilin, V., 2002. Anaerobic Digestion Model No 1 (ADM1). IWA Publishing, London, UK.

Batstone, D.J., Keller, J., Newell, R.B., Newland, M., 2000a. Modelling anaerobic degradation of complex wastewater. I: Model development. Bioresource Technol. 75, 67–74.

Batstone, D.J., Keller, J., Newell, R.B., Newland, M., 2000b. Modelling anaerobic degradation of complex wastewater. II: Parameter estimation and validation using slaughterhouse effluent. Bioresource Technol. 75, 75–85.

Bernard, O., Hadj-Sadok, Z., Dochain, D., Genovesi, A., Steyer, J.-P., 2001. Dynamical model development and parameter identification for an anaerobic wastewater treatment process. Biotechnol. Bioeng. 75, 424–438.

Degenring, D., Frömel, C., Dikta, G., Takors, R., 2004. Sensitivity analysis for the reduction of complex metabolism models. J. Proc. Control 14, 729–745.

Dochain, D., Vanrolleghem, P.A., 2001. Dynamical Modelling and Estimation in Wastewater Treatment Processes. IWA Publishing, London, UK.

Kesavan, P., Law, V.J., 2005. Practical identifiability of parameters in Monod kinetics and statistical analysis of residuals. Biochem. Eng. J. 24, 95–104.

Lou, S.J., Tartakovsky, B., Zeng, Y., Wu, P., Guiot, S.R., 2006. Fluorescence-based monitoring of tracer and substrate distribution in an UASB reactor. Chemosphere 65, 1212–1220.

Makinia, J., Wells, S., 2000. A general model of the activated sludge reactor with dispersive flow - I. Model development and parameter estimation. Wat. Res. 34, 3987–3996.

Morel, E., Santamaria, K., Perrier, M., Guiot, S.R., Tartakovsky, B., 2004. Application of multi-wavelength fluorometry for on-line monitoring of an anaerobic digestion process. Wat. Res. 38, 3287–3296.

Mshandete, A., Murto, M., Kivaisi, A.K., Rubindamayugi, M.S.T., Mattiasson, B., 2004. Influence of recirculation flow rate on the performance of anaerobic packed-bed bioreactors treating potato-waste leachate. Env. Technol. 25, 929–936.

Mu, S.J., Zeng, Y., Wu, P., Lou, S.J., Tartakovsky, B., 2008. Anaerobic digestion model No. 1-based distributed parameter model of an anaerobic reactor: I. Model development. Bioresource Technol. 99, 3665–3675.

Nelder, J.A., Mead, R., 1965. A simplex method for function minimization. Comput. J. 7, 308–313.

Rosen, C., Jeppsson, U., 2002. Anaerobic COST benchmark model description. Dept of Industrial Electrical Engineering and Automation. Lund University, Lund, Sweden.

Sam-Soon, P., Loewenthal, R.E., Wentzel, M.C., Moosbrugger, R.E., 1991. Effects of a recycle in upflow anaerobic sludge bed (UASB) systems. Water SA 17, 37–45.

Torkian, A., Eqbali, A., Hashemian, S.J., 2003. The effect of organic loading rate on the performance of UASB reactor treating slaughterhouse effluent. Resour. Conserv. Recy. 40, 1–11.

Zeng, Y., Mu, S.J., Lou, S.J., Tartakovsky, B., Guiot, S.R., Wu, P., 2005. Hydraulic modeling and axial dispersion analysis of UASB reactor. Biochem. Eng. J. 25, 113–123.